Gas and Mode, Vertical and Rotational Effects with a Three Piston Gauge Apparatus

J. W. Schmidt, B. E. Welch and C. D. Ehrlich

Abstract. A semi-automated three piston gauge apparatus has been used to measure gas species and mode effects in a low pressure pneumatic dead-weight piston gauge. Two gases, He and N_2, were used in both gauge and absolute modes, as well as several "intermediate" modes, to characterize a single gauge. The results of the measurements are compared with a model for crevice effects that incorporates both molecular and viscous flow regimes. The model has previously been applied to spin decay rate measurements on the four gases He, N_2, H_2 and SF_6, and has now been extended to account for differences in effective area arising from species changes. Mode effects remain that cannot be predicted by the model.

1. Introduction

The pneumatic piston gauge has continued to develop and to be refined as a pressure measurement device for more than forty years. It consists of a hollow cylinder oriented vertically in which is placed a close-fitting piston, pressurized from below and sometimes evacuated from above. Pressure is then measured (or generated) by loading the piston with known masses until the piston floats freely between upper and lower limits. Over time the precision and estimated accuracy of piston gauges has improved so that, at present, these gauges can measure/generate relative pressures in some cases with a precision 1×10^{-6} or 2×10^{-6}.

However, recently a number of researchers have documented species effects in gas operated piston gauges, in some cases at the 30×10^{-6} level, and mode effects at the 25×10^{-6} level [1-4]. These effects are thought to be due to forces that are not completely understood which act on the piston in the region of the crevice. In the present work we have tried to provide further evidence for these two effects under controlled conditions, and to explain some of the observations in a typical cross-float situation with a simple model. We have already met with some success in explaining rotational spin-rate decay measurements, in which we examined both species and mode effects, by employing a phenomenological model for forces in the piston/cylinder crevice that bridges the two relevant flow regimes (viscous and molecular). That model, described in a previous publication [5], covers azimuthal or circumferential forces and is now extended to cover the vertical forces encountered in cross-float situations. The extended model works well in accounting for experimentally-observed absolute-mode species effects but only marginally accounts for gauge to absolute mode effects. Other explanations for the gauge to absolute mode effects may be needed. The present measurements were taken with the aid of a Three Piston Gauge Apparatus (TPGA) under development at the NIST.

J. W. Schmidt, B. E. Welch and C. D. Ehrlich: Thermophysics Division, National Institute of Standards and Technology, Gaithersburg, MD 20899, USA.

2. Model: Forces in the Crevice

We have previously used a model for circumferential forces in the crevice between the piston and cylinder that works well for spin-time measurements [5] using four gases (He, H_2, N_2 and SF_6) as the working fluids. The essential feature of the model is that it uses a simple interpolation function $f(\lambda/h)$ between the viscous and molecular-flow regimes as a momentum transfer function,

$$f(\lambda/h) \simeq \frac{\eta}{1+\lambda/h}. \qquad (1)$$

metrologia

Metrologia 1993/94, **30**, 599-602

Here η is the gas dynamic viscosity and λ/h is the ratio of the molecular mean free path to the crevice width. The resulting forces in the transition regime are represented by analytic functions of λ/h that match smoothly onto the corresponding forces in the viscous and molecular-flow regimes.

We have now extended the model to include the vertical forces which must be known if accurate pressure measurements are to be obtained. The present model [6] predicts that the effective area of a piston gauge is

$$A_{\text{eff}} \equiv \pi R_0^2 + \pi h R_0 \left[1 + \frac{8(8/\pi - 3)\beta}{P_1 - P_0} \ln\left(\frac{P_1 + 24\beta}{P_0 + 24\beta} \right) \right], \quad (2)$$

where R_0 is the radius of the piston, h is the crevice width between piston and cylinder, P_0 and P_1 are the absolute pressures above and below the piston, $\beta = \eta kT/M\bar{c}h$,, where k is Boltzmann's constant, T is the temperature of the gas, M is the molecular mass, and $\bar{c}$ is the mean molecular speed. The dependence of the model on species occurs through the term involving β, which depends on η and M, and is thus different for each gas. The mode dependence occurs because A_{eff} depends separately on P_1 and P_0, not just on the difference $P_1 - P_0$. Note that the simple viscous flow model [7] is independent of both species and pressure and is represented by the first two terms $\pi R_0^2 + \pi h R_0$ on the right side of (2).

3. A Three Piston Gauge Apparatus

Measurements were taken using the TPGA of which the essential arrangement is shown schematically in Figure 1. Two calibrated reference gauges were used to check the pressures above and below a test gauge. Reference gauge #1 (PG-29, a transfer standard) was calibrated against a primary standard Hg manometer over the range 15 kPa to 100 kPa in the absolute mode [1,2]. With the arrangement in Figure 1, absolute pressures at both the top and bottom of the test gauge could be determined precisely. Absolute pressures in the bell jars of the reference gauges were measured to ± 1,0 Pa with thermocouple gauges. However, the difference in the bell-jar pressures of the reference gauges were measured with respect to each other to within ± 0,026 Pa (0,2 μHg) with a calibrated (and frequently zeroed) differential capacitance diaphragm gauge (CDG). The combined uncertainty affects the measurement of the effective area with a relative uncertainty of less than $1{,}0 \times 10^{-6}$. The differences in absolute pressures between gauge #1 and the test gauge were also measured with a calibrated (and frequently zeroed) differential capacitance diaphragm gauge. The rms pressure fluctuations indicated by the CDG were typically less than $10^{-6} \times P_1$.

Piston heights were measured using inductive proximity sensors beneath the weight hangers. In operation, each of these measurements was taken four times/minute

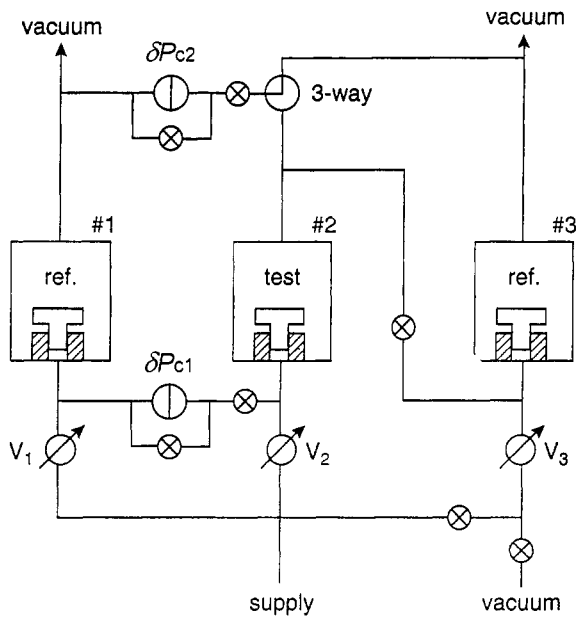

Figure 1. Schematic representation of the three piston gauge apparatus.

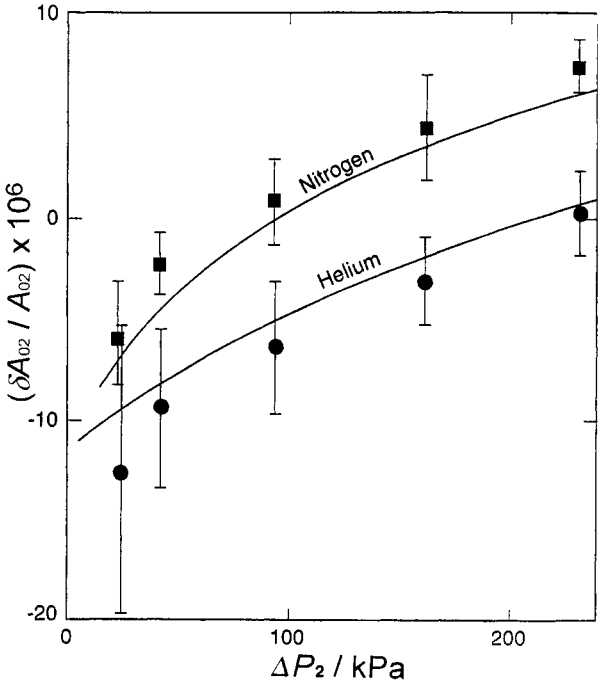

Figure 2. Change in effective area of test gauge # 2 versus applied pressure in the absolute mode. Change is expressed as $\delta A_{02}/A_{02}$ where A_{02} is 3,357 08 cm^2 and $\delta A_{02} = A_{\text{eff}} - A_{02}$.

and used in a proportional, integral and differential feedback loop to control the piston height at the required reference levels. Gas leaking past each piston was replaced with the aid of valves controlled by a desktop computer. Valves of two types were used, a motorized needle valve and two precision piezoelectric valves. Setting up a cross-float under feedback control, then shutting down the control valves, changed the apparent balance condition $\delta P_{cdg}/(P_1 - P_0)$ by less than 10^{-6}.

4. Measurements and Discussion

Figure 2 shows the change in absolute mode effective areas A_{eff} of test gauge #2 versus the differential pressure $\Delta P = P_1 - P_0$. The data were obtained from a standard two piston cross-float of the test gauge against reference gauge #1. Two pressurizing gases were used: He and N_2. The effective areas A_{eff} were calculated for each set of conditions using the equation

$$\frac{\sum m_i g(1-\rho_2/\rho_i)}{A_{eff}(1+\alpha_2\delta T_2)(1+b_2\Delta P_2)} = \Delta P_1(T_1) + \delta P_{c1} - \delta P_{c2} + PH_{12}, \quad (3)$$

where $m_i g(1-\rho_2/\rho_i)$ represents the buoyancy corrected weights, m_i and ρ_i are the individual masses and densities of the weights, g is the local acceleration due to gravity, ρ_2 is the density of the gas above the piston (negligible in the absolute mode), α_2 and b_2 are the thermal expansion and pressure coefficients of the test gauge, δT_2 is the difference in T_2 from the reference temperature, ΔP_2 is the pressure generated by the test gauge, ΔP_1 (T_1) is the pressure generated by reference gauge #1 at temperature T_1, δP_{c1} and δP_{c2} are the readings taken from the differential pressure cells shown in Figure 1 (operating near to but not necessarily at null), and the last term PH_{12} is the pressure head correction.

Clear, non-zero slopes in the data plotted in Figure 2 can be seen for both gases and there is an offset between the two gases. This is consistent with the present model which predicts both of these features. The two sets of data also appear to exhibit slight negative curvatures, which is again consistent with the model. The solid lines were calculated using the model described earlier (2) with the crevice width h fixed at 1,61 μm. This value for h was obtained in previous rotational measurements [5] as a fitting parameter and is within tolerances given by the manufacturer. The only adjustable parameter in fitting (2) to the data in Figure 2 was R_0, which could, in principle, be measured independently.

Figure 3 shows data taken in the three piston mode in which gauge #3 served to generate the reference pressure for the top side of the test gauge. Effective areas A_{eff} were calculated using a simple extension of the previous equation:

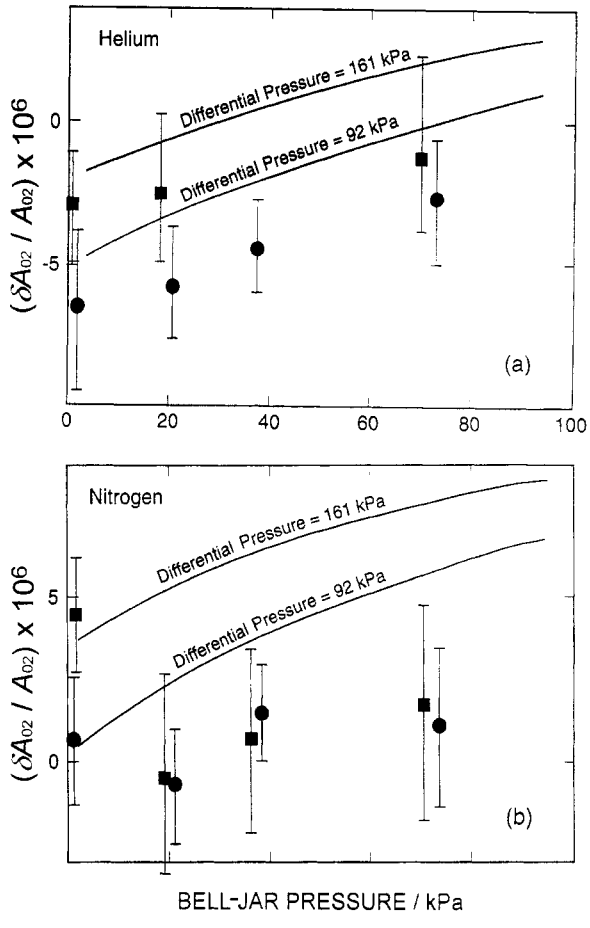

Figure 3. (a) Change in effective area of test gauge # 2 versus bell-jar pressure using helium throughout. Circles represent a loading of the test gauge of about 92 kPa; squares represent a loading of about 161 kPa. Solid lines represent the model described in the text for the two loads. (b) Same as (a) but with nitrogen used throughout.

$$\frac{\sum m_i g(1-\rho_2/\rho_i)}{A_{eff}(1+\alpha_2\delta T_2)(1+b_2\Delta P_2)} = \Delta P_1(T_1) - \Delta P_3(T_3) + \delta P_{c1} - \delta P_{c2} + PH_{12} - PH_{23}, \quad (4)$$

where $\Delta P_3(T_3)$ is the recorded pressure of gauge #3 at temperature T_3 and PH_{23} is an extra head correction for the line connecting the test gauge and gauge #3. We have also included in Figure 3 lines which represent the present model with the same parameters as used in Figure 2.

The model remains a plausible explanation for the He data shown in Figure 3a. As predicted, the squares, which represent the higher loads, are generally above the circles which represent lower loads, and the data appear to increase monatonically with bell-jar pressure, also as predicted. In the case of N_2, shown in Figure 3b, the agreement is not as good. The data appear to decrease at

first and then rise as bell-jar pressure increases. The model, however, predicts that the effective area should increase monotonically, by about 6×10^{-6} times the geometric piston area, for a typical load. We are not yet sure of the cause of the small discrepancy between the data and the model but are investigating the possibility that the piston may tilt within the crevice in the absolute mode because of the relative reduction in restoring forces at the top of the piston. This would increase [8] the effective area, possibly significantly, in the absolute mode, in contrast with the present model. Finally, we observe that the data in Figures 3a and 3b show increased scatter with respect to Figure 2 owing to the increased complexity of the measurements. Note, however, that a systematic error of only 5×10^{-6} would produce the disagreement shown in Figure 3b.

5. Summary

We have measured gas species and mode effects on the effective area of a low pressure pneumatic dead-weight piston gauge. A model for the gas flow in the crevice ($h = 1{,}61$ μm) used above to explain spin decay rates has now been extended in an attempt to explain the gas species effect. While the model works well in explaining the species effect for He and N_2 in the absolute mode, it predicts a mode effect that is not clearly discernable in the present gauge-mode data. We are attempting to improve the resolution of a three piston gauge apparatus to sort out these effects. Measurements are currently under way on other gauges in which larger effects have been seen.

Acknowledgements. This work was supported by the US Air Force under contract CCG-910A038, Task 319.

References

1. Welch B. E., Edsinger R. E., Bean V. E., Ehrlich C. D., High Pressure Metrology (Edited by G. F. Molinar), *BIPM Monographie 89*, 1989, 81.
2. Welch B. E., Edsinger R. E., Bean V. E., Ehrlich C. D., *J. Res. NIST*, 1989, **94**, 343.
3. Tilford C. R., Hyland R. W., Sheng Yi-tang, High Pressure Metrology (Edited by G. F. Molinar), *BIPM Monographie 89*, 1989, 105.
4. Meyer C. W., Reilly M. L., In *Temperature: Its Measurement and Control in Science and Industry*, Vol. 6 (Edited by J. F. Schooley), New York, American Institute of Physics, 1992, 133.
5. Schmidt J. W., Welch B. E., Ehrlich C. D., *Meas. Sci. Technol.*, 1993, **4**, 26.
6. Schmidt J. W., Welch B. E., Ehrlich C. D., in preparation.
7. Landau L. P., Lifshitz E. M., *Fluid Mechanics*, Vol. 6, London, Pergamon, 1959.
8. Dadson R. S., Lewis S. L., Peggs G. N., *The Pressure Balance – Theory and Practice*, London, HMSO, 1982.